

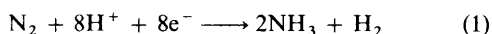
Comparative Study on the Multielectron Reduction of $\text{HOC}_2\text{H}_4\text{N}_3$ catalyzed by $[\text{NBu}^n_4]_4[\text{MoFe}_3\text{S}_4(\text{SPh})_3(o\text{-O}_2\text{C}_6\text{Cl}_4)]_2^-$ and $[\text{NBu}^n_4]_2[\text{Fe}_4\text{S}_4(\text{SPh})_4]$ -modified Glassy Carbon Electrodes

Koji Tanaka,* Satoshi Uezumi, and Toshio Tanaka

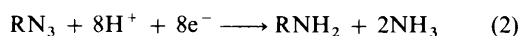
Department of Applied Chemistry, Faculty of Engineering, Osaka University, Yamada-oka, Suita, Osaka 565, Japan

Both $[\text{NBu}^n_4]_4[\text{MoFe}_3\text{S}_4(\text{SPh})_3(o\text{-O}_2\text{C}_6\text{Cl}_4)]_2^-$ and $[\text{NBu}^n_4]_2[\text{Fe}_4\text{S}_4(\text{SPh})_4]$ -modified glassy carbon electrodes ($[\text{MoFe}]/\text{GC}$ and $[\text{4Fe}]/\text{GC}$, respectively) can catalyse the multielectron reduction of $\text{HOC}_2\text{H}_4\text{N}_3$ to afford not only $\text{HOC}_2\text{H}_4\text{NH}_2$ and N_2 but also N_2H_4 and NH_3 in water. The six- and eight-electron reduction products N_2H_4 and NH_3 are formed *via* an unstable four-electron reduction product N_2H_2 . The catalytic ability of $[\text{MoFe}]/\text{GC}$ is much superior to that of $[\text{4Fe}]/\text{GC}$ with respect to such multielectron reduction.

Nitrogenase is composed of iron-sulphur and molybdenum-iron proteins, and the latter plays the central role in the eight-electron reduction of N_2 affording 2 mol of NH_3 and 1 mol of H_2 ¹ [equation (1)]. The molybdenum-iron protein contains



Fe_4S_4 and $\text{MoFe}_{6-8}\text{S}_{8-9}$ clusters,² and the reduction of N_2 is believed to take place on the Mo atom of the $\text{MoFe}_{6-8}\text{S}_{8-9}$ cluster, though any direct evidence for this has not been provided so far. The reduction of nitrogenase substrates by synthetic FeS and MoFeS clusters, therefore, is of much interest in the elucidation of the functions of Fe_4S_4 and $\text{MoFe}_{6-8}\text{S}_8$ clusters in the molybdenum-iron protein. The lack of any synthetic FeS and MoFeS clusters having a strong affinity for N_2 , however, makes it difficult to simulate nitrogenase reactions. This problem may be overcome provided N_2 is concentrated on those clusters. It is well known that organic azides (RN_3) are subject to bond breaking between the RN and N_2 moieties.³ By taking advantage of this reactivity, RN_3 has been used as a starting material for the preparation not only of nitrene complexes⁴ but also of dinitrogen metal complexes.⁵ It is, therefore, possible to concentrate N_2 on FeS and MoFeS clusters by the two-electron reduction of RN_3 on those clusters. Consequently, if a system which can transport electrons to the clusters successively can be constructed, RN_3 may undergo eight-electron reduction affording 2 mol of NH_3 *via* N_2 together with 1 mol of RNH_2 [equation (2)]. Along these lines we have



reported an electrochemical eight-electron reduction of RN_3 ($\text{R} = \text{Me}$ or $\text{C}_2\text{H}_4\text{OH}$) with a triply bridged double cubane MoFeS cluster, $[\text{Mo}_2\text{Fe}_6\text{S}_8(\text{SPh})_9]^{3-}$, at modified glassy carbon plates, where RN_3 co-ordinates to the Fe atom of the reduced species of the cluster.⁶ The multi-electron reduction of RN_3 co-ordinated to the Mo atom of MoFeS clusters is also of interest in connection with the active site of nitrogenase.

This paper describes a comparative study on the catalytic activity of the molybdenum and iron sites of the single cubane MoFe_3S_4 and Fe_4S_4 clusters, respectively, toward the multi-electron reduction of $\text{HOC}_2\text{H}_4\text{N}_3$ in water.

Experimental

Materials.—Commercially available guaranteed reagent grades of NaOH, H_3PO_4 , and $\text{HOCH}_2\text{CH}=\text{CH}_2$ were used

without further purification. Solvents were purified by distillation over dehydration chemicals, P_2O_5 for MeCN and CaO for *N,N*-dimethylformamide (dmf). All solvents were stored under N_2 . Immediately before use they were bubbled with He for 1 h to remove N_2 dissolved in the solvents. The molybdenum-iron-sulphur cluster $[\text{NBu}^n_4]_4[\text{MoFe}_3\text{S}_4(\text{SPh})_3(o\text{-O}_2\text{C}_6\text{Cl}_4)]_2^-$,⁷ the iron-sulphur cluster $[\text{NBu}^n_4]_2[\text{Fe}_4\text{S}_4(\text{SPh})_4]$,⁸ and $\text{HOC}_2\text{H}_4\text{N}_3$ ⁹ were prepared according to the literature methods. The cluster-modified glassy carbon electrodes were prepared by addition of a given amount of an acetonitrile solution (1.0×10^{-3} mol dm^{-3}) of $[\text{NBu}^n_4]_4[\text{MoFe}_3\text{S}_4(\text{SPh})_3(o\text{-O}_2\text{C}_6\text{Cl}_4)]_2^-$ or $[\text{NBu}^n_4]_2[\text{Fe}_4\text{S}_4(\text{SPh})_4]$ to a polished surface of the glassy carbon plates (1.0 and 3.0 cm^2) by syringe techniques and followed by drying for *ca.* 30 min under dry N_2 .⁶ The electrodes thus prepared were used for the electrochemical measurements and the reduction of $\text{HOC}_2\text{H}_4\text{N}_3$ in water.

Physical Measurements.—Electronic absorption spectra were measured with a Union SM-401 spectrophotometer. The equilibrium constant (K) between $[\text{MoFe}_3\text{S}_4(\text{SPh})_3(o\text{-O}_2\text{C}_6\text{Cl}_4)(\text{dmf})]^{2-}$ and $\text{HOC}_2\text{H}_4\text{N}_3$ in dmf was obtained from the change in absorbance at 470 nm of the charge-transfer (c.t.) band of the former in the presence of various amounts of $\text{HOC}_2\text{H}_4\text{N}_3$ by using equation (3), where d_0 , d , and d_∞ are the

$$d = \frac{d_0 - d}{[\text{HOC}_2\text{H}_4\text{N}_3]K} + d_\infty \quad (3)$$

absorbances of the initial concentration of $[\text{MoFe}_3\text{S}_4(\text{SPh})_3(o\text{-O}_2\text{C}_6\text{Cl}_4)(\text{dmf})]^{2-}$, the equilibrium mixture of the latter and $\text{HOC}_2\text{H}_4\text{N}_3$, and $[\text{MoFe}_3\text{S}_4(\text{SPh})_3(o\text{-O}_2\text{C}_6\text{Cl}_4)(\text{N}_3\text{C}_2\text{H}_4\text{OH})]^{2-}$, respectively. Spectroelectrochemical experiments were performed by using an optically transparent thin-layer electrode (OTTLE), described elsewhere.¹⁰ Cyclic voltammograms were obtained by the use of a Hokuto Denko potentiostat HB-401, a Hokuto Denko function generator HB-107, and a Yokogawa Electric X-Y recorder 3077.

Reduction of $\text{HOC}_2\text{H}_4\text{N}_3$ with the Cluster-modified Glassy Carbon Electrodes.—The reduction of $\text{HOC}_2\text{H}_4\text{N}_3$ was carried out under controlled-potential electrolysis conditions using an electrolysis cell consisting of three compartments:¹¹ one for a cluster-modified glassy carbon electrode, the second for a

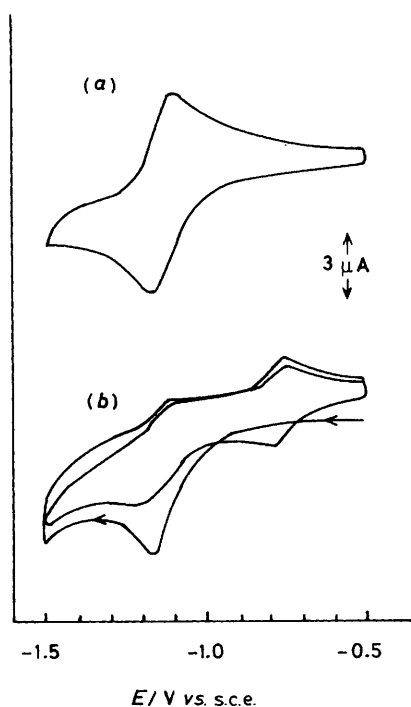


Figure 1. Cyclic voltammogram of $[\text{NBu}_4]_2[\text{MoFe}_3\text{S}_4(\text{SPh})_3(o\text{-O}_2\text{C}_6\text{Cl}_4)(\text{dmf})]^{2-}$ ($1.8 \times 10^{-3} \text{ mol dm}^{-3}$) in the absence (a) and presence of $\text{HOC}_2\text{H}_4\text{N}_3$ ($0.9 \times 10^{-3} \text{ mol dm}^{-3}$) (b) in dmf; sweep rate 100 mV s^{-1} , glassy carbon electrode

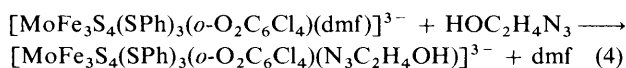
platinum counter electrode, which was separated from the former by a cation-exchange membrane (Nafion film), and the third for a saturated calomel electrode (s.c.e.) as reference. The volumes of these compartments were 45, 30, and 10 cm^3 , respectively, and the first two were connected to volumetric flasks with stainless-steel tubes (0.4 mm inside diameter). After flushing the cell with He, an aqueous buffer solution ($\text{NaOH-H}_3\text{PO}_4$, 0.5 mol dm^{-3}) was introduced into each compartment and $\text{HOC}_2\text{H}_4\text{N}_3$ was then injected into the working electrode cell by syringe techniques. The electrolysis cell was placed in a thermostat at 30°C , and the solution in the cell was stirred magnetically for 0.5 h. The reduction of $\text{HOC}_2\text{H}_4\text{N}_3$ was started by applying a fixed potential to the cluster-modified glassy carbon electrode with a potentiostat. The charge consumed in the reduction was measured with a Hokuto Denko HF-201 coulometer.

Product Analysis.—The volume of the gas evolved in the reduction of $\text{HOC}_2\text{H}_4\text{N}_3$ was determined from the change in the meniscus of water in a volumetric flask connected to the working electrode cell. At a fixed interval, 0.1-cm^3 portions of gas were sampled with a pressure-lock syringe (Precision Sampling) from the gaseous phase not only in the working electrode compartment but also in the volumetric flask, through septum caps attached to the top of those compartments. Gas analysis was performed on a Shimadzu gas chromatograph GC-3BT. The analysis of the reactant and products in the solution was performed at a fixed interval by sampling 0.1-cm^3 portions of the solution in the working electrode cell with syringe techniques through a septum cap. In order to liberate free amine and ammonia the solution taken from the cell was mixed with an aqueous NaOH saturated solution ($1.0 \times 10^{-5} \text{ dm}^3$) in a sealed tube with a septum cap. Then, the resulting alkaline solutions were analysed with Shimadzu gas chromatographs GC-6A and GC-7A. The details of the analytical conditions were

described in a previous paper.⁶ The amount of N_2H_4 was determined by spectrophotometric titration.¹²

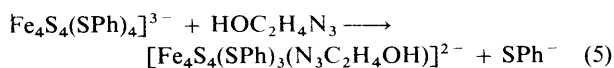
Results and Discussion

Cyclic Voltammograms of $[\text{MoFe}_3\text{S}_4(\text{SPh})_3(o\text{-O}_2\text{C}_6\text{Cl}_4)]_2^{4-}$ and $[\text{Fe}_4\text{S}_4(\text{SPh})_4]^{2-}$ in dmf.—The doubly bridged double cubane MoFeS cluster $[\text{MoFe}_3\text{S}_4(\text{SR})_3(o\text{-O}_2\text{C}_6\text{Cl}_4)]_2^{4-}$ ($\text{R} = \text{alkyl and aryl}$) dissociates into two single cubane clusters $[\text{MoFe}_3\text{S}_4(\text{SR})_3(o\text{-O}_2\text{C}_6\text{Cl}_4)(\text{solvent})]^{2-}$ in polar solvents such as dmf, MeCN, Me_2CO , and tetrahydrofuran (thf) by co-ordination of those solvents to the molybdenum atom and cleavage of two Fe-S(R)-Mo bridging bonds; the solvated molecules are substituted by various substrates such as PR_3 , RS^- , N_3^- , and NH_2NH_2 to afford the 1:1 adduct.⁷ Similar adduct formation between $[\text{MoFe}_3\text{S}_4(\text{SPh})_3(o\text{-O}_2\text{C}_6\text{Cl}_4)(\text{dmf})]^{2-}$ and $\text{HOC}_2\text{H}_4\text{N}_3$ was observed in the cyclic voltammogram in dmf: $[\text{MoFe}_3\text{S}_4(\text{SPh})_3(o\text{-O}_2\text{C}_6\text{Cl}_4)(\text{dmf})]^{2-}$ shows one cathodic and one anodic wave at -1.16 and $-1.09 \text{ V vs. s.c.e.}$, respectively [Figure 1(a)]. The addition of $\text{HOC}_2\text{H}_4\text{N}_3$ to this solution hardly affects the voltammogram in the first cathodic scanning from -0.50 to -1.50 V , the cathodic wave at -1.16 V having essentially the same peak current as that in the absence of $\text{HOC}_2\text{H}_4\text{N}_3$. In the reverse anodic scanning, however, the peak current of the anodic wave at -1.09 V becomes weak; instead a new anodic wave appears at -0.70 V . The second scanning shows a new cathodic wave at -0.76 V and the peak current of the original cathodic wave at -1.16 V becomes weak [Figure 1(b)]. Thus, the cyclic voltammogram of $[\text{MoFe}_3\text{S}_4(\text{SPh})_3(o\text{-O}_2\text{C}_6\text{Cl}_4)(\text{dmf})]^{2-}$ in the presence of $\text{HOC}_2\text{H}_4\text{N}_3$ exhibits two reversible redox couples at $E_{\frac{1}{2}} [(E_{pc} + E_{pa})/2] = -1.13$ and $-0.73 \text{ V vs. s.c.e.}$ after the second scanning. The peak current of the redox couple at $E_{\frac{1}{2}} = -0.73 \text{ V}$ is increased with increasing amount of $\text{HOC}_2\text{H}_4\text{N}_3$ added, while that of the original redox couple at $E_{\frac{1}{2}} = -1.13 \text{ V}$ gradually decreases. The former increase in the peak current almost ceased when more than 1.0 equivalent of $\text{HOC}_2\text{H}_4\text{N}_3$ was added. These results clearly indicate that the adduct formation between $[\text{MoFe}_3\text{S}_4(\text{SPh})_3(o\text{-O}_2\text{C}_6\text{Cl}_4)(\text{dmf})]^{2-}$ and $\text{HOC}_2\text{H}_4\text{N}_3$ hardly takes place under the present experimental conditions, while the reduced cluster $[\text{MoFe}_3\text{S}_4(\text{SPh})_3(o\text{-O}_2\text{C}_6\text{Cl}_4)(\text{dmf})]^{3-}$ reacts with $\text{HOC}_2\text{H}_4\text{N}_3$ to form the 1:1 adduct, $[\text{MoFe}_3\text{S}_4(\text{SPh})_3(o\text{-O}_2\text{C}_6\text{Cl}_4)(\text{N}_3\text{C}_2\text{H}_4\text{OH})]^{3-}$ [equation (4)], for which $E_{\frac{1}{2}} (3-/2-) = -0.73 \text{ V vs. s.c.e.}$ It should be noted that the substitution of dmf



at the Mo atom of the MoFe_3S_4 core by $\text{HOC}_2\text{H}_4\text{N}_3$ (see below) resulted in an anodic shift of the $E_{\frac{1}{2}}$ value of the cluster by about 400 mV, suggesting a decrease in the electron density of the MoFe_3S_4 core upon adduct formation with $\text{HOC}_2\text{H}_4\text{N}_3$.

The cyclic voltammogram of $[\text{Fe}_4\text{S}_4(\text{SPh})_4]^{2-}$ in dmf shows cathodic and anodic waves at -1.06 and -0.99 V [Figure 2(a)]. The peak currents of those redox couples were not changed by the addition of a 5 molar excess of $\text{HOC}_2\text{H}_4\text{N}_3$ even in the multi-scanning cyclic voltammograms. On the other hand, when $[\text{Fe}_4\text{S}_4(\text{SPh})_4]^{2-}$ existing around the electrode was reduced to $[\text{Fe}_4\text{S}_4(\text{SPh})_4]^{3-}$ by applying a potential of -1.30 V to the electrode for 3 min a new redox couple appears at $E_{pa} = -1.07$ and $E_{pc} = -1.13 \text{ V}$ as shoulders on the original redox couple at $E_{\frac{1}{2}} = -1.03 \text{ V}$ [Figure 2(b)]. The new redox couple at $E_{\frac{1}{2}} = -1.10 \text{ V}$ may be associated with the $(2-/1-)$ redox couple of $[\text{Fe}_4\text{S}_4(\text{SPh})_3(\text{N}_3\text{C}_2\text{H}_4\text{OH})]^{2-}$ resulting from a slow adduct formation between $[\text{Fe}_4\text{S}_4(\text{SPh})_4]^{3-}$ and $\text{HOC}_2\text{H}_4\text{N}_3$ [equation (5)] (see below). Thus, both $[\text{Fe}_4\text{S}_4(\text{SPh})_4]^{3-}$ and



$[\text{MoFe}_3\text{S}_4(\text{SPh})_3(o\text{-O}_2\text{C}_6\text{Cl}_4)(\text{dmf})]^{3-}$ react with $\text{HOC}_2\text{H}_4\text{N}_3$ to form the corresponding adducts. It is noteworthy that the E_3 value of the $[\text{Fe}_4\text{S}_4(\text{SPh})_3(\text{N}_3\text{C}_2\text{H}_4\text{OH})]^{1-/2-}$ couple is shifted

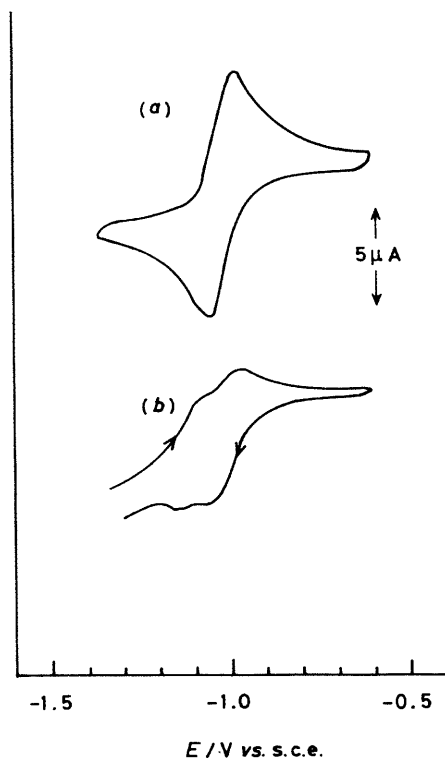


Figure 2. Cyclic voltammogram of $[\text{NBu}_4]_2[\text{Fe}_4\text{S}_4(\text{SPh})_4]$ (1.8×10^{-3} mol dm^{-3}) (a) and after applying -1.30 V *vs.* s.c.e. to the glassy carbon electrode for 3 min in the presence of $\text{HOC}_2\text{H}_4\text{N}_3$ (9.0×10^{-3} mol dm^{-3}) (b) in dmf; sweep rate 100 mV s^{-1} , glassy carbon electrode

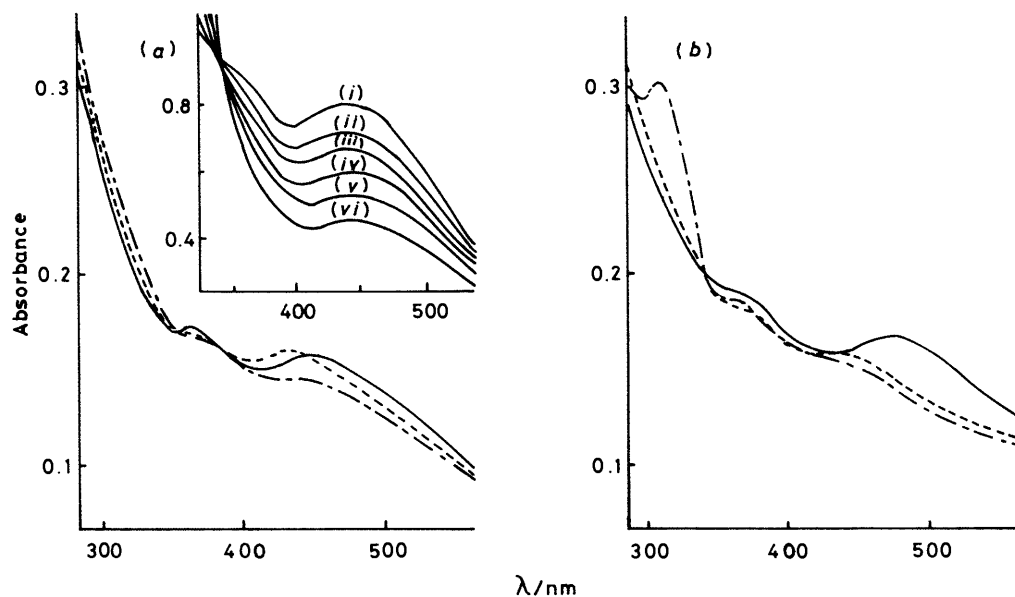
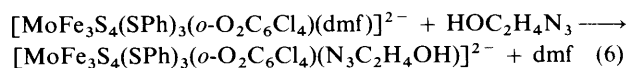


Figure 3. Electronic absorption spectra of $[\text{MoFe}_3\text{S}_4(\text{SPh})_3(o\text{-O}_2\text{C}_6\text{Cl}_4)(\text{dmf})]^{2-}$ (a) and $[\text{Fe}_4\text{S}_4(\text{SPh})_4]^{2-}$ (b) (—, 1.0×10^{-4} mol dm^{-3}), and the reduced species prepared at -1.10 V *vs.* s.c.e. in the absence (---) and the presence of $\text{HOC}_2\text{H}_4\text{N}_3$ (- · - ·, 2.0×10^{-4} mol dm^{-3}) in dmf. Inset: the spectral change of $[\text{MoFe}_3\text{S}_4(\text{SPh})_3(o\text{-O}_2\text{C}_6\text{Cl}_4)(\text{dmf})]^{2-}$ (6.0×10^{-4} mol dm^{-3}) in the presence of 0 (i), 6.0×10^{-3} (ii), 1.20×10^{-2} (iii), 2.40×10^{-2} (iv), 4.20×10^{-2} (v), and 7.20×10^{-2} mol dm^{-3} $\text{HOC}_2\text{H}_4\text{N}_3$, (vi)

cathodically by 70 mV compared with that of the $[\text{Fe}_4\text{S}_4(\text{SPh})_4]^{3-/2-}$ couple. Thus, the substitution of PhS^- in $[\text{Fe}_4\text{S}_4(\text{SPh})_4]^{3-}$ by $\text{HOC}_2\text{H}_4\text{N}_3$ results in an increase in electron density of the Fe_4S_4 core.

Interaction of $[\text{MoFe}_3\text{S}_4(\text{SPh})_3(o\text{-O}_2\text{C}_6\text{Cl}_4)(\text{dmf})]^{3-}$ and $[\text{Fe}_4\text{S}_4(\text{SPh})_4]^{3-}$ with $\text{HOC}_2\text{H}_4\text{N}_3$.—Although adduct formation between $[\text{MoFe}_3\text{S}_4(\text{SPh})_3(o\text{-O}_2\text{C}_6\text{Cl}_4)(\text{dmf})]^{2-}$ and $\text{HOC}_2\text{H}_4\text{N}_3$ was not observed in the cyclic voltammograms, the c.t. band (470 nm) of $[\text{NBu}_4]_2[\text{MoFe}_3\text{S}_4(\text{SPh})_3(o\text{-O}_2\text{C}_6\text{Cl}_4)(\text{dmf})]$ in dmf gradually changed on addition of a large excess of $\text{HOC}_2\text{H}_4\text{N}_3$ to given an isosbestic point at 350 nm [insert in Figure 3(a)]. Thus, the oxidized cluster $[\text{MoFe}_3\text{S}_4(\text{SPh})_3(o\text{-O}_2\text{C}_6\text{Cl}_4)(\text{dmf})]^{2-}$ also forms an adduct with $\text{HOC}_2\text{H}_4\text{N}_3$ [equation (6)] in the presence of a large excess of $\text{HOC}_2\text{H}_4\text{N}_3$.*



The equilibrium constant of equation (6) calculated from the change in the absorbance at 470 nm was 30 ± 2 $\text{dm}^3 \text{mol}^{-1}$ at 25°C . As expected from such a small equilibrium constant, the electronic absorption spectrum of $[\text{NBu}_4]_2[\text{MoFe}_3\text{S}_4(\text{SPh})_3(o\text{-O}_2\text{C}_6\text{Cl}_4)(\text{dmf})]$ (1.0×10^{-4} mol dm^{-3}) in dmf [Figure 3(a)] was essentially unchanged in the presence of a 2 molar excess of $\text{HOC}_2\text{H}_4\text{N}_3$. Controlled-potential electrolysis of this solution at -1.10 V *vs.* s.c.e. in dmf causes a blue shift of the band at 470 nm to 450 nm and a decrease in absorption coefficient [— · — in Figure 3(a)], apparently different from that of $[\text{MoFe}_3\text{S}_4(\text{SPh})_3(o\text{-O}_2\text{C}_6\text{Cl}_4)(\text{dmf})]^{3-}$ [— — — in Figure 3(a)] prepared under the same electrolysis conditions but in the absence of $\text{HOC}_2\text{H}_4\text{N}_3$. Despite this difference in the electronic spectra,

* The cyclic voltammogram of $[\text{MoFe}_3\text{S}_4(\text{SPh})_3(o\text{-O}_2\text{C}_6\text{Cl}_4)(\text{N}_3\text{C}_2\text{H}_4\text{OH})]^{2-}$ in dmf containing a large excess of $\text{HOC}_2\text{H}_4\text{N}_3$ showed a strong cathodic current at potentials more negative than -0.90 V *vs.* s.c.e. due to the reduction of $\text{HOC}_2\text{H}_4\text{N}_3$ co-ordinated to $[\text{MoFe}_3\text{S}_4(\text{SPh})_3(o\text{-O}_2\text{C}_6\text{Cl}_4)(\text{N}_3\text{C}_2\text{H}_4\text{OH})]^{3-}$ with the hydroxy proton of $\text{HOC}_2\text{H}_4\text{N}_3$ in the solution.

reoxidation of the solutions at -0.60 V regenerated the electronic spectrum of $[\text{MoFe}_3\text{S}_4(\text{SPh})_3(o\text{-O}_2\text{C}_6\text{Cl}_4)(\text{dmf})]^{2-}$. Thus, one-electron reduction of $[\text{MoFe}_3\text{S}_4(\text{SPh})_3(o\text{-O}_2\text{C}_6\text{Cl}_4)(\text{dmf})]^{2-}$ greatly enhances the affinity for $\text{HOC}_2\text{H}_4\text{N}_3$, as similarly to that for CO .⁷ The lack of an absorption band arising from free PhS^- (see below) in the electronic absorption spectrum of $[\text{MoFe}_3\text{S}_4(\text{SPh})_3(o\text{-O}_2\text{C}_6\text{Cl}_4)(\text{dmf})]^{3-}$ in the presence of $\text{HOC}_2\text{H}_4\text{N}_3$ suggests that $\text{HOC}_2\text{H}_4\text{N}_3$ co-ordinates to the Mo rather than to the Fe of the MoFe_3S_4 core.

In contrast to the electronic absorption spectrum of the $[\text{MoFe}_3\text{S}_4(\text{SPh})_3(o\text{-O}_2\text{C}_6\text{Cl}_4)(\text{dmf})]^{2-}$ - $\text{HOC}_2\text{H}_4\text{N}_3$ system, the c.t. band of $[\text{Fe}_4\text{S}_4(\text{SPh})_4]^{2-}$ in dmf at 470 nm was not changed at all even after an addition of a 100 molar excess of $\text{HOC}_2\text{H}_4\text{N}_3$ [— in Figure 3(b)]. Thus, $[\text{Fe}_4\text{S}_4(\text{SPh})_4]^{2-}$ has essentially no interaction with $\text{HOC}_2\text{H}_4\text{N}_3$. On the other hand, the electronic absorption spectrum of $[\text{Fe}_4\text{S}_4(\text{SPh})_4]^{3-}$ prepared by controlled-potential electrolysis of $[\text{Fe}_4\text{S}_4(\text{SPh})_4]^{2-}$ at -1.30 V in the presence of a 2 molar excess of $\text{HOC}_2\text{H}_4\text{N}_3$ [· — in Figure 3(b)] is markedly different from that obtained in the absence of $\text{HOC}_2\text{H}_4\text{N}_3$ [— in Figure 3(b)]. The absorption band at 306 nm appeared only in the presence of $\text{HOC}_2\text{H}_4\text{N}_3$ and is assigned to PhS^- ; the absorption coefficient corresponds to 1 mol of PhS^- dissociated from $[\text{Fe}_4\text{S}_4(\text{SPh})_4]^{3-}$. Upon reoxidation of the cluster at -0.60 V the electronic spectrum of $[\text{Fe}_4\text{S}_4(\text{SPh})_4]^{2-}$ was almost completely recovered even in the presence of $\text{HOC}_2\text{H}_4\text{N}_3$. This result indicates that one of the terminal PhS^- ligated to $[\text{Fe}_4\text{S}_4(\text{SPh})_4]^{3-}$ is substituted by $\text{HOC}_2\text{H}_4\text{N}_3$ [equation (5)], similar to the reaction of $[\text{Fe}_4\text{S}_4(\text{SPh})_4]^{3-}$ with $n\text{-C}_5\text{H}_{11}\text{N}_3$.¹³

Cyclic Voltammogram of the Cluster-modified Glassy Carbon Electrode in Water.—Similarly to the triply bridged double cubane MoFeS cluster $[\text{NBu}_4]_3[\text{Mo}_2\text{Fe}_6\text{S}_8(\text{SPh})_9]$,⁶ not only $[\text{NBu}_4]_4[\text{MoFe}_3\text{S}_4(\text{SPh})_3(o\text{-O}_2\text{C}_6\text{Cl}_4)_2]$ but also $[\text{NBu}_4]_2[\text{Fe}_4\text{S}_4(\text{SPh})_4]$ modified on glassy carbon plates ($[\text{MoFe}]/\text{GC}$ and $[\text{4Fe}]/\text{GC}$, respectively) undergo stable redox reactions in water: the cyclic voltammogram of $[\text{MoFe}]/\text{GC}$ in water at pH 10.0 is exemplified in Figure 4, which shows an anodic wave at -0.89 V vs. s.c.e. and a strong cathodic current at potentials more negative than -1.0 V due not only to the reduction of the cluster modified on the glassy carbon plate but also to the evolution of H_2 catalysed by the reduced species of the cluster (— in Figure 4). The cathodic current consumed in the reduction of the cluster can be separated from that for evolution of H_2 by subtracting the cathodic currents in the cathodic scan from the anodic scan⁶ (— — in Figure 4). The number of coulombs consumed in the cathodic wave at -1.15 V thus obtained is consistent with that in the anodic wave at -0.89 V vs. s.c.e., and corresponds to one electron per MoFe_3S_4 core. This result indicates that almost all clusters modified undergo redox reaction on the glassy carbon plate. The cyclic voltammogram of $[\text{4Fe}]/\text{GC}$ also exhibited an anodic wave corresponding to the $[\text{Fe}_4\text{S}_4(\text{SPh})_4]^{3-/2-}$ couple at -0.84 V and a strong cathodic current at potentials more negative than -1.10 V due to evolution of H_2 catalysed by the reduced species of the cluster. Subtracting the cathodic currents in the cathodic sweep from the anodic one also afforded the cathodic wave of the $[\text{Fe}_4\text{S}_4(\text{SPh})_4]^{3-/2-}$ redox couple at -1.18 V.

The peak separation ΔE_p ($E_{pa} - E_{pc}$) of $[\text{MoFe}]/\text{GC}$ (260 mV) and $[\text{4Fe}]/\text{GC}$ (340 mV) is larger than that in dmf. It is worth noting that the latter value is almost consistent with the ΔE_p (350 mV) of the (2-/3-) redox couple of $[\text{Fe}_4\text{S}_4(\text{SPh})_4]^{2-}$ ($E_{1/2} = -1.34$ V vs. s.c.e.) attached covalently to a tin oxide electrode in dmf.¹⁴ The ΔE_p values of the adsorbed species is frequently used as a criterion for kinetics in the electron transfer between the electrode and the redox site. Thus, for rapid kinetics

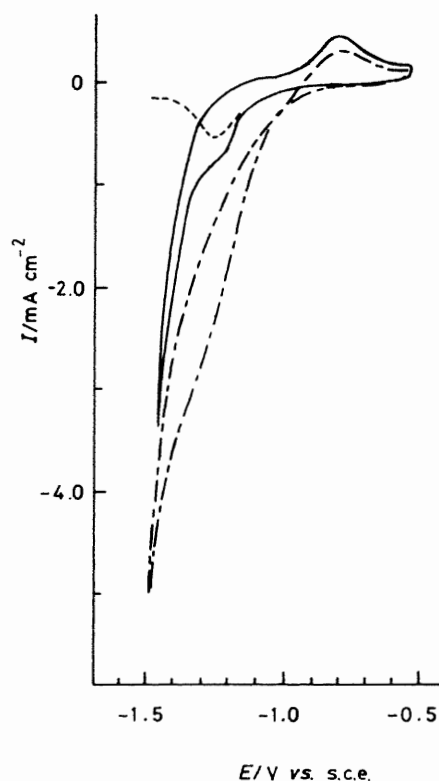


Figure 4. Cyclic voltammograms of $[\text{MoFe}]/\text{GC}$ (5.0×10^{-8} mol) in the absence (—) and presence of $\text{HOC}_2\text{H}_4\text{N}_3$ (1.2×10^{-2} mol dm^{-3}) (---) in an aqueous buffer solution at pH 10.0; the cathodic wave (- · -) was obtained by subtracting the cathodic currents in the anodic sweep from the anodic one in the absence of $\text{HOC}_2\text{H}_4\text{N}_3$.

$\Delta E_p = 0$ is expected at any scan rate.¹⁵ If the electron transfer is slow, both anodic and cathodic peak potentials are dependent on the scan rate, and ΔE_p increases with decreasing electron transfer.¹⁵ In the present study, the form of the cluster of $[\text{MoFe}]/\text{GC}$ and $[\text{4Fe}]/\text{GC}$ largely influences the electron transfer since these clusters exist essentially in the solid state. For charge neutrality, the redox reaction of the clusters on the glassy carbon plates requires the transport of the counter ion from the contacting electrolyte solution into the space of the clusters modified on the carbon plate. This process may retard the electron transfer in the modified electrode compared with that in dmf solution. In accordance with this, the cyclic voltammograms of both $[\text{4Fe}]/\text{GC}$ and $[\text{MoFe}]/\text{GC}$ did not show the redox couples of the clusters when a bulky electrolyte NBu_4Br was used in place of $\text{NaOH-H}_3\text{PO}_4$ buffer as an aqueous electrolyte. In addition, the energy barrier to a conformational change of the clusters between the oxidized⁸ and reduced forms¹⁶ accompanying the redox reaction in the solid state may be larger than that in solution. The large peak separation of $[\text{MoFe}]/\text{GC}$ and $[\text{4Fe}]/\text{GC}$ (ΔE_p 260 and 340 mV), therefore, may be caused mainly not only by the permeability of the counter ion in the crystal lattice of the clusters but also by the conformational changes in the solid state.

The stability of the cluster-modified carbon electrode is largely dependent on the solubility of the counter ions in water since the redox reaction of the cluster results in the transport of the counter ion from and to the contacting electrolyte solution. Such a counter ion movement in the modified electrodes, more or less, accelerates the detachment of the clusters from the carbon plates. The anodic peak currents of the NEt_4^+ salts of $[\text{MoFe}_3\text{S}_4(\text{SPh})_3(o\text{-O}_2\text{C}_6\text{Cl}_4)_2]^{4-}$ and $[\text{Fe}_4\text{S}_4(\text{SPh})_4]^{2-}$

Table. Reduction of RN_3 ($\text{R} = \text{C}_2\text{H}_4\text{OH}$) catalysed by $[\text{MoFe}]/\text{GC}$ and $[\text{4Fe}]/\text{GC}$ ^a in water (16 cm^3) at $\text{pH } 10$ ^b

Entry	Electrode	E/V <i>vs. s.c.e.</i>	Amount of $\text{RN}_3/\mu\text{mol}$	pH	Products/ μmol					
					H_2	N_2	RNH_2	RNHNH_2	NH_3	N_2H_4
1	[MoFe]/GC	-1.25	200	10	36.7	164	174	13.6	36.6	Trace
2		-1.25	100	10	21.1	84.1	89.1	6.8	15.0	Trace
3		-1.25	200 ^c	10	16.9	114	115	19.3	20.1	0
4		-1.10	200	10	Trace	123	127	7.6	10.5	Trace
5		-1.10	200	8	10	130	141	31.7	55.3	Trace
6	[4Fe]/GC	-1.10	250	12	0	135	140	0	0	0
7		-1.25	100	10	25.1	64.7	71.1	0	10.4	0.33
8		-1.25	100 ^c	10	10.6	54.9	56.0	0	0	0
9		-1.10	100 ^d	10	0	94.7	95.9	0	0	0

^a 5.0×10^{-8} mol. ^b For 4 h. ^c $\text{HOCH}_2\text{CH}=\text{CH}_2$ (1.6×10^{-3} mol) was added. ^d For 24 h.

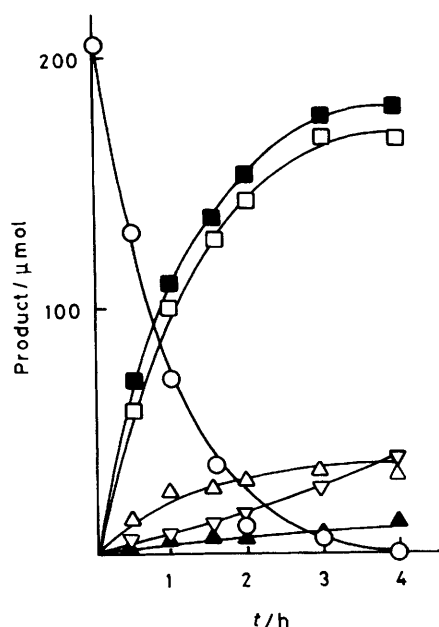
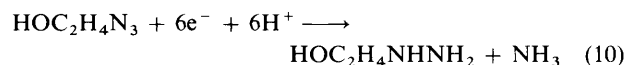
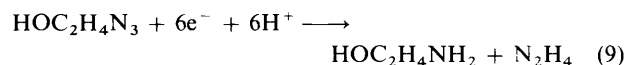


Figure 5. Reduction of $\text{HOC}_2\text{H}_4\text{N}_3$ (O) (1.20×10^{-2} mol dm^{-3}) by $[\text{MoFe}]/\text{GC}$ (5.0×10^{-8} mol) upon controlled-potential electrolysis at -1.25 V *vs. s.c.e.* in an aqueous buffer solution at $\text{pH } 10$. Products: (■) RNH_2 , (□) N_2 , (△) NH_3 , (▽) H_2 , and (▲) RN_2H_3

modified on carbon plates* were gradually weakened in the multi-scanning cyclic voltammograms and almost disappeared in 30 min, while the decrease of the anodic peak currents of the NBu_4^+ salts of the cluster-modified electrode ($[\text{MoFe}]/\text{GC}$ and $[\text{4Fe}]/\text{GC}$) was 20% in the multi-scanning cyclic voltammograms for 1 h. Thus, the NBu_4^+ salt of the cluster-modified electrode is much better than the NEt_4^+ salt with respect to the stability of the electrode. This may be due to the lower solubility of NBu_4^+ than NEt_4^+ in water. In addition, the anodic peak currents of $[\text{MoFe}]/\text{GC}$ and $[\text{4Fe}]/\text{GC}$ in the cyclic voltammograms obtained after controlled-potential electrolysis at -1.25 V *vs. s.c.e.* in water ($\text{pH } 10$) for 3 h were essentially unchanged from the peak currents measured in the cyclic voltammograms in the initial stage. Such a great improvement of the stability of both $[\text{MoFe}]/\text{GC}$ and $[\text{4Fe}]/\text{GC}$ results from the decrease in the movement of the counter ions in the cluster-modified electrode under the

conditions of controlled-potential electrolysis. The catalytic behaviours of the MoFeS and FeS clusters upon reduction of $\text{HOC}_2\text{H}_4\text{N}_3$, therefore, were examined by using the NBu_4^+ salts of these clusters on glassy carbon plates. Both modified electrodes work as efficient catalysts in the reduction of $\text{HOC}_2\text{H}_4\text{N}_3$ in water; the cathodic current of $[\text{MoFe}]/\text{GC}$ increases upon addition of $\text{HOC}_2\text{H}_4\text{N}_3$ to the aqueous phase compared with that in the absence of $\text{HOC}_2\text{H}_4\text{N}_3$ (— in Figure 4). The current density at -1.25 V *vs. s.c.e.* in the presence of $\text{HOC}_2\text{H}_4\text{N}_3$ (1.2×10^{-2} mol dm^{-3}) is about three times larger than that in its absence. The cathodic current density of $[\text{4Fe}]/\text{GC}$ in the cathodic sweep in the presence of $\text{HOC}_2\text{H}_4\text{N}_3$ (1.2×10^{-2} mol dm^{-3}) was also about 2.7 times larger than that in the absence of $\text{HOC}_2\text{H}_4\text{N}_3$ at -1.25 V *vs. s.c.e.* in water ($\text{pH } 10.0$).

Reduction of $\text{HOC}_2\text{H}_4\text{N}_3$ with $[\text{MoFe}]/\text{GC}$ and $[\text{4Fe}]/\text{GC}$.—Controlled-potential electrolysis of $[\text{MoFe}]/\text{GC}$ at -1.25 V *vs. s.c.e.* in water ($\text{pH } 10.0$) in the presence of $\text{HOC}_2\text{H}_4\text{N}_3$ affords not only $\text{HOC}_2\text{H}_4\text{NH}_2$ and N_2 but also $\text{HOC}_2\text{H}_4\text{NHNH}_2$, N_2H_4 (trace),[†] and NH_3 together with H_2 (Figure 5). The amount of H_2 evolved in the reduction increased with decreasing amount of $\text{HOC}_2\text{H}_4\text{N}_3$ used (entries 1 and 2 in the Table). Thus, protons and $\text{HOC}_2\text{H}_4\text{N}_3$ are reduced competitively with $[\text{MoFe}]/\text{GC}$ according to reactions (7)–(10). In

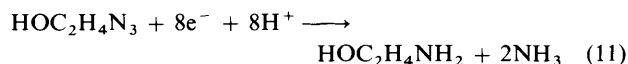


addition to these, the eight-electron reduction (11) affording $\text{HOC}_2\text{H}_4\text{NH}_2$ and NH_3 is considered to take place at the same time from the facts that the amount of NH_3 formed is 2.4–2.7 times larger than that of $\text{HOC}_2\text{H}_4\text{NHNH}_2$ [equation (10)]

[†] Spectrophotometric titration of N_2H_4 was affected by the presence of $\text{HOC}_2\text{H}_4\text{NHNH}_2$ since both N_2H_4 and $\text{HOC}_2\text{H}_4\text{NHNH}_2$ exhibit an absorption band at 458 nm in aqueous acidic *p*-dimethylaminobenzaldehyde solution.¹² The band position in the aqueous solution shifted to 480 (N_2H_4) and 465 nm ($\text{HOC}_2\text{H}_4\text{NHNH}_2$) in ethanolic solution. The ethanolic titration solution prepared from the reaction mixture showed the band at 480 nm as a shoulder on the band at 465 nm, but the band intensity of the former was too weak for quantitative analysis of N_2H_4 .

* The anodic and cathodic peak potentials of the NEt_4^+ salts of MoFeS and FeS cluster-modified electrodes are completely consistent with those of the NBu_4^+ salts of the clusters ($[\text{MoFe}]/\text{GC}$ and $[\text{4Fe}]/\text{GC}$).

(entries 1 and 2 in the Table) and that $\text{HOC}_2\text{H}_4\text{N}_3$ is not reduced at all with $[\text{MoFe}]/\text{GC}$ under the same electrolysis conditions.* The six- and eight-electron reductions affording

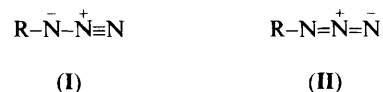


N_2H_4 and NH_3 [equations (9) and (11)], respectively, may proceed *via* preliminary cleavage of the $\text{HOC}_2\text{H}_4\text{N}-\text{N}_2$ bond due to two-electron reduction [equation (8)], suggesting the involvement of a four-electron-reduction intermediate such as N_2H_2 , which is considered as a reaction intermediate in dinitrogen reduction by nitrogenase. Schrauzer *et al.*¹⁷ have reported that N_2H_2 formed as a reaction intermediate in their models of nitrogen fixation by oxomolybdenum complexes is trapped by olefin molecules, inhibiting the formation of N_2H_4 and NH_3 completely. On the other hand, the reduction of $\text{HOC}_2\text{H}_4\text{N}_3$ with $[\text{MoFe}]/\text{GC}$ in the presence of $\text{HOCH}_2\text{-CH}=\text{CH}_2$ as a trap for N_2H_2 still produced NH_3 together with $\text{HOC}_2\text{H}_4\text{NHNH}_2$, $\text{HOC}_2\text{H}_4\text{NH}_2$, N_2 , and H_2 . It should, however, be noted that the amount of NH_3 is decreased compared with that formed in the absence of $\text{HOCH}_2\text{CH}=\text{CH}_2$ (compare entries 1 and 3 in the Table). In addition, almost equal amounts not only of $\text{HOC}_2\text{H}_4\text{NHNH}_2$ and NH_3 [equation (10)] but also of $\text{HOC}_2\text{H}_4\text{NH}_2$ and N_2 [equation (8)] were formed (entry 3 in the Table). This result suggests that only the reductions (8) and (10) occur in the presence of $\text{HOCH}_2\text{-CH}=\text{CH}_2$, and the other six- and eight-electron reductions affording N_2H_4 [equation (9)] and NH_3 [equation (11)] are almost completely inhibited by $\text{HOCH}_2\text{CH}=\text{CH}_2$. The difference in the amounts between NH_3 and $\text{HOC}_2\text{H}_4\text{NHNH}_2$, therefore, corresponds to the amount of NH_3 formed in the eight-electron reduction (11). The six- and eight-electron reductions are also largely influenced not only by the electrode potentials but also by the proton concentrations in water; an anodic shift of the $[\text{MoFe}]/\text{GC}$ potential from -1.25 to -1.10 V resulted in a considerable decrease in the formation of NH_3 (compare entry 1 with entry 4 in the Table). Furthermore, the amount of NH_3 decreased with increasing pH in controlled-potential electrolysis at -1.10 V and neither NH_3 nor $\text{HOC}_2\text{H}_4\text{NHNH}_2$ was formed at pH 12.0 (entries 4–6 in the Table). It is, therefore, concluded that not only a rapid electron transfer to the cluster but also high proton concentrations are required to catalyse the multielectron reduction of $\text{HOC}_2\text{H}_4\text{N}_3$.†

The reduction of $\text{HOC}_2\text{H}_4\text{N}_3$ with $[\text{4Fe}]/\text{GC}$ by controlled-potential electrolysis at -1.25 V *vs.* s.c.e. also produced $\text{HOC}_2\text{H}_4\text{NH}_2$, N_2 , N_2H_4 , and NH_3 , but $\text{HOC}_2\text{H}_4\text{NHNH}_2$ was not identified at all in the reaction mixture (entry 7 in the Table). In accordance with this, the summation of the current efficiency for the formation of $\text{HOC}_2\text{H}_4\text{NH}_2$, N_2 , N_2H_4 , and NH_3 based on the stoichiometries of equations (8), (9), and (11) was 100% within experimental errors ($\pm 1.0\%$). The same reduction conducted in the presence of $\text{HOCH}_2\text{CH}=\text{CH}_2$ as a trap for a possible intermediate N_2H_2 produced only equal amounts of $\text{HOC}_2\text{H}_4\text{NH}_2$ and N_2 [equation (8)], and neither N_2H_4 [equation (9)] nor NH_3 [equation (11)] was formed (entry 8 in the Table). Thus, the formation of N_2H_4 and NH_3 in the reduction of $\text{HOC}_2\text{H}_4\text{N}_3$ with $[\text{4Fe}]/\text{GC}$ may also involve a

preliminary cleavage of the $\text{HOC}_2\text{H}_4\text{N}-\text{N}_2$ bond. The catalytic ability of $[\text{4Fe}]/\text{GC}$ toward multielectron reduction of $\text{HOC}_2\text{H}_4\text{N}_3$ is less than that of $[\text{MoFe}]/\text{GC}$ since $[\text{4Fe}]/\text{GC}$ catalyses only the two-electron reduction of $\text{HOC}_2\text{H}_4\text{N}_3$ affording equal amounts of $\text{HOC}_2\text{H}_4\text{NH}_2$ and N_2 [equation (8)] by controlled-potential electrolysis at -1.10 V (entry 9 in the Table), while $[\text{MoFe}]/\text{GC}$ catalyses not only two- [equation (8)] but also six- [equation (9) and (10)] and eight-electron reduction [equation (11)] of $\text{HOC}_2\text{H}_4\text{N}_3$ under the same electrolysis conditions.

Pathway of the Reduction of $\text{HOC}_2\text{H}_4\text{N}_3$.—Organic azides are considered to exist mainly as resonance form (I) rather than (II), since the bond distance between the 'RN' and 'N₂' moieties



of RN_3 is always longer than that between the 'RN₂' and 'N' moieties,¹⁸ and protonation of RN_3 in strong acidic media occurs in the resonance form (I).¹⁹ Consequently, organic azides preferentially co-ordinate to metals with the nitrogen atom adjacent to the organic group²⁰ and usually undergo bond breaking between the 'RN' and 'N₂' moieties to afford nitrene⁴ and dinitrogen complexes.⁵ Such a preferential bond cleavage also takes place in the present study since about 75 and 85% of the electrons transferred to $[\text{MoFe}]/\text{GC}$ and $[\text{4Fe}]/\text{GC}$, respectively, are consumed in the two-electron reduction of $\text{HOC}_2\text{H}_4\text{N}_3$ [equation (8)] by controlled-potential electrolysis at -1.25 V *vs.* s.c.e. in water at pH 10.0. The reduction of $\text{HOC}_2\text{H}_4\text{N}_3$ is initiated by its co-ordination to the clusters of $[\text{MoFe}]/\text{GC}$ and $[\text{4Fe}]/\text{GC}$ since neither proton nor $\text{HOC}_2\text{-H}_4\text{N}_3$ is reduced with a glassy carbon plate under the present electrolysis conditions. On the basis of the fact that the six- and eight-electron reductions [equations (9) and (11)] are completely inhibited by $\text{HOCH}_2\text{CH}=\text{CH}_2$, part of the N_2 formed in the two-electron reduction of $\text{HOC}_2\text{H}_4\text{N}_3$ [equation (8)] may undergo further successive reductions on these clusters to afford N_2H_4 and NH_3 [equations (9) and (11)] *via* a possible intermediate N_2H_2 . The affinity of the present clusters for N_2 , however, is very weak since a decrease in the electron flow to the cluster by an anodic shift of the $[\text{4Fe}]/\text{GC}$ potential from -1.25 to -1.10 V *vs.* s.c.e. resulted in complete inhibition of the formation of N_2H_4 and NH_3 (entry 9 in the Table). Accordingly, the formation of NH_3 and N_2H_4 upon controlled-potential electrolysis of $[\text{MoFe}]/\text{GC}$ at -1.10 V manifests the superiority of $[\text{MoFe}]/\text{GC}$ over $[\text{4Fe}]/\text{GC}$ in the multielectron reduction of $\text{HOC}_2\text{H}_4\text{N}_3$. The rate of electron transfer between the carbon plate and the cluster in the modified electrode may be slower than that in the corresponding homogeneous system, as described in a previous section. However, controlled-potential electrolysis at -1.25 V *vs.* s.c.e. of an MeOH - thf solution (1:1 v/v) containing $[\text{NBu}_4]_4[\text{MoFe}_3\text{S}_4(\text{SPh})_3(o\text{-O}_2\text{C}_6\text{Cl}_4)_2]$ or $[\text{NBu}_4]_2[\text{Fe}_2\text{S}_4(\text{SPh})_4]$ (1.0 mmol dm^{-3}), $\text{HOC}_2\text{H}_4\text{N}_3$ (0.10 mol dm^{-3}), and LiCl produced only equal amounts of $\text{HOC}_2\text{H}_4\text{NH}_2$ and N_2 with a current efficiency of 100%. The inability of the MoFeS and FeS clusters to facilitate multielectron reduction of $\text{HOC}_2\text{H}_4\text{N}_3$ in an homogeneous solution may result from the lack of a system which can transport electrons to the cluster continuously. Thus, the cluster-modified electrodes are endowed with the ability of catalysing multielectron reduction of $\text{HOC}_2\text{H}_4\text{N}_3$ [equations (9)–(11)].

The striking difference between $[\text{MoFe}]/\text{GC}$ and $[\text{4Fe}]/\text{GC}$ is the ability and inability to catalyze the six-electron reduction of $\text{HOC}_2\text{H}_4\text{N}_3$ affording $\text{HOC}_2\text{H}_4\text{NHNH}_2$ and NH_3 [equation

* Controlled-potential electrolysis of an aqueous solution of $\text{HOC}_2\text{H}_4\text{NHNH}_2$ (2×10^{-2} mol dm^{-3}) with $[\text{MoFe}]/\text{GC}$ and $[\text{4Fe}]/\text{GC}$ in water (pH 10.0) at -1.25 V *vs.* s.c.e. produced only H_2 with a current efficiency of 100%.

† When the reduction of $\text{HOC}_2\text{H}_4\text{N}_3$ was carried out at pH 6.0 by electrolysis at -1.25 V *vs.* s.c.e., vigorous evolution of H_2 disrupted the cluster coating on the glassy carbon electrode, resulting in a decrease in the rate of reduction.

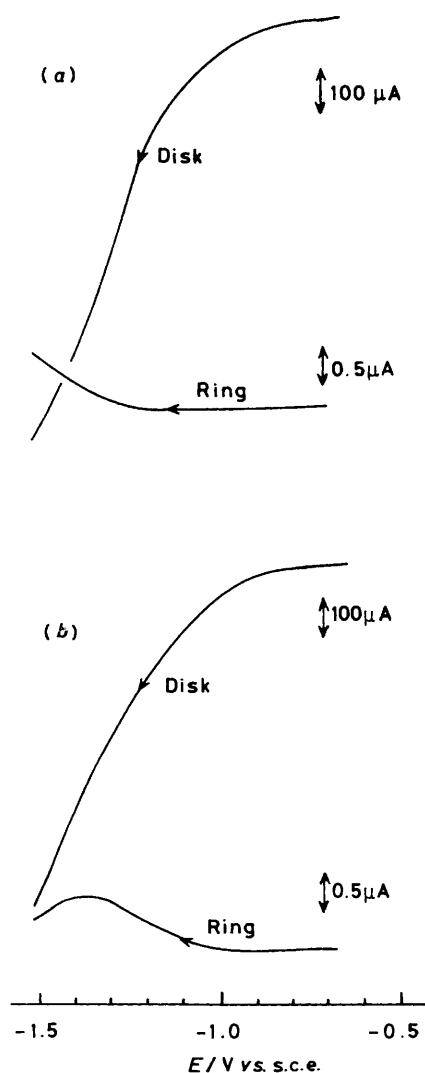


Figure 6. Current curves of the disk and ring electrodes *vs.* potentials of [MoFe]/GC (a) and [4Fe]/GC (b) (4×10^{-9} mol) in water (pH 10.0) containing $\text{HOC}_2\text{H}_4\text{N}_3$ (0.20 mol dm^{-3}). The potential of the ring electrode was $+0.40 \text{ V}$, $dE/dt = 10 \text{ mV s}^{-1}$, and $\omega = 1000 \text{ revolutions min}^{-1}$

(10)]. In contrast to the reaction pathways (8), (9), and (11), $\text{HOC}_2\text{H}_4\text{NHNH}_2$ is formed by elimination of the terminal nitrogen from $\text{HOC}_2\text{H}_4\text{N}_3$. The most probable precursor for $\text{HOC}_2\text{H}_4\text{NHNH}_2$ may be a $(\text{NH}=\text{N}=\text{N}-\text{C}_2\text{H}_4\text{OH})-\text{MoFeS}$ cluster adduct. Several triazenometal complexes have been prepared so far by insertion of aryl azides into metal-hydride bonds of complexes of Re, W,²¹ Os,²² and Hf.²³ In harmony with this, the formation of $\text{HOC}_2\text{H}_4\text{NHNH}_2$ is accompanied by evolution of H_2 (entries 1–5 in the Table), suggesting that a similar insertion of $\text{HOC}_2\text{H}_4\text{N}_3$ into a hydride cluster as a precursor for evolution of H_2 takes place in the reduction of $\text{HOC}_2\text{H}_4\text{N}_3$ with [MoFe]/GC. The superiority of [MoFe]/GC over [4Fe]/GC may be associated with the difference in the sites of co-ordination of $\text{HOC}_2\text{H}_4\text{N}_3$ to those clusters. Although the Mo atom of the MoFe_3S_4 core in the solid state is co-ordinatively saturated,⁷ $\text{HOC}_2\text{H}_4\text{N}_3$ may preferentially bind to the Mo atom in the MoFe_3S_4 core by cleaving one of the bridging Mo–SPh–Fe bonds at least, by analogy with the adduct formation in dmf solution. On the other hand, $\text{HOC}_2\text{H}_4\text{N}_3$ co-ordinates to the Fe atom by substitution of a

terminal PhS^- ligand of the Fe_4S_4 core. These assumptions suggest that the reduction of $\text{HOC}_2\text{H}_4\text{N}_3$ with [MoFe]/GC is not accompanied by dissociation of PhS^- from the MoFeS cluster, while the same reduction with [4Fe]/GC causes PhS^- to dissociate from the FeS cluster. The reduction of $\text{HOC}_2\text{H}_4\text{N}_3$, therefore, was conducted by using an rotating ring-disk electrode (r.r.d.e.),⁶ in which only the glassy carbon disk electrode is modified with $[\text{NBu}_4][\text{MoFe}_3\text{S}_4(\text{SPh})_3(o\text{-O}_2\text{C}_6\text{-Cl}_4)_2]$ or $[\text{NBu}_4]_2[\text{Fe}_4\text{S}_4(\text{SPh})_4]$ and the potential of the glassy carbon ring electrode fixed at $+0.40 \text{ V}$ in order to detect PhS^- liberated from the disk electrode.⁶ In the first cathodic sweep (10 mV s^{-1}) of the [MoFe]/GC disk electrode potential (E_d) from -0.6 to $-1.5 \text{ V vs. s.c.e.}$ with rotation of the r.r.d.e. at $\omega = 1000 \text{ revolutions min}^{-1}$ in the presence of $\text{HOC}_2\text{H}_4\text{N}_3$ in water at pH 10.0 the cathodic current (I_d) of [MoFe]/GC increases at E_d more negative than -1.0 V due to the reduction of $\text{HOC}_2\text{H}_4\text{N}_3$ and protons [upper line of Figure 6(a)]. At the same time, the anodic current of the ring electrode (I_r) resulting from the oxidation of PhS^- begins to increase at E_d more negative than $-1.30 \text{ V vs. s.c.e.}$ as shown in the lower line of Figure 6(a), which clearly shows that the substitution of PhS^- ligated on the Fe atom of the MoFeS cluster essentially does not take place at E_d more positive than -1.30 V . The reduction of $\text{HOC}_2\text{H}_4\text{N}_3$ with the [4Fe]/GC modified disk electrode of the r.r.d.e. ($1000 \text{ revolutions min}^{-1}$) in water also results in an increase in the cathodic current of I_d at E_d more negative than -1.0 V [upper line of Figure 6(b)]. However, the I_r due to the oxidation of PhS^- increases at E_d more negative than -1.0 V and then decreases at E_d more negative than -1.40 V [lower line of Figure 6(b)]. Thus, the reduction of $\text{HOC}_2\text{H}_4\text{N}_3$ with [4Fe]/GC causes dissociation of PhS^- from the FeS cluster and the substitution of PhS^- of the FeS cluster by $\text{HOC}_2\text{H}_4\text{N}_3$ occurs in the initial stage. In addition, the MoFe_3S_4 and Fe_4S_4 cores on the glassy carbon plates may be essential for catalysis of the reduction of $\text{HOC}_2\text{H}_4\text{N}_3$ since the same reduction by NEt_4^+ salts of the MoFeS and FeS cluster-modified electrodes in place of the corresponding NBu_4^+ salts almost ceased in 1 h due to the detachment of the salts from the carbon plates. This result seems to rule out the possibility that the reduction of $\text{HOC}_2\text{H}_4\text{N}_3$ is catalyzed by the decomposition products of the MoFeS and FeS clusters. As the active site of the nitrogenase model reaction, Mo, therefore, appears to be more suitable than Fe. This may result from the fact that the Mo of the MoFe_3S_4 core is a stronger electron donor to $\text{HOC}_2\text{H}_4\text{N}_3$ than is Fe of the Fe_4S_4 core.

References

- H. Dalton and L. E. Mortenson, *Bacteriol. Rev.*, 1972, 231; L. E. Mortenson and R. N. F. Thorneley, *Annu. Rev. Biochem.*, 1979, **48**, 387.
- M. J. Nelson, M. A. Lery, and W. H. Orme-Johnson, *Proc. Natl. Acad. Sci. U.S.A.*, 1983, **80**, 147; S. S. Yang, W. H. Pan, G. D. Friesen, B. K. Burgess, J. L. Corbin, E. I. Stiefel, and W. E. Newton, *J. Biol. Chem.*, 1982, 257, 8042.
- F. Rolla, *J. Org. Chem.*, 1982, **47**, 4327; S. N. Maiti, M. P. Singh, and R. G. Micetich, *Tetrahedron Lett.*, 1986, **27**, 1423; S. C. Shim and K. N. Choi, *ibid.*, 1985, **26**, 3277.
- L. G. Hubert-Pfalgraf and G. Aharonian, *Inorg. Chim. Acta*, 1985, **100**, L21; R. S. Dickson, R. J. Nesbit, H. Pateras, W. Baimbridge, J. M. Patrick, and A. H. White, *Organometallics*, 1985, **4**, 2128; J. H. Osborne, A. L. Rheingold, and W. C. Trogler, *J. Am. Chem. Soc.*, 1985, **107**, 7945; J. H. Osborne and W. C. Trogler, *Inorg. Chem.*, 1985, **24**, 3098.
- J. P. Collman, M. Kubota, J. Sun, and F. Vastine, *J. Am. Chem. Soc.*, 1967, **89**, 169; B. Bell, J. Chatt, and G. J. Leigh, *J. Chem. Soc., Dalton Trans.*, 1973, 997.
- S. Kuwabata, K. Tanaka, and T. Tanaka, *Inorg. Chem.*, 1986, **25**, 1691.
- W. H. Armstrong, P. K. Maschark, and R. H. Holm, *J. Am. Chem. Soc.*, 1982, **104**, 4373; P. K. Maschark, W. H. Armstrong, Y. Mizobe,

- and R. H. Holm, *ibid.*, 1983, **105**, 475; R. E. Palermo, R. Singh, J. K. Bashkin, and R. H. Holm, *ibid.*, 1984, **106**, 2600.
- 8 L. Que, jun., M. A. Bobrik, J. A. Ibers, and R. H. Holm, *J. Am. Chem. Soc.*, 1974, **4186**, 96.
- 9 O. Pimroth and W. Wislicenus, *Ber. Dtsch. Chem. Ges.*, 1905, **38**, 1573.
- 10 D. Lexa, J. M. Savent, and J. J. Zickler, *J. Am. Chem. Soc.*, 1977, **99**, 2786.
- 11 K. Tanaka, M. Honjo, and T. Tanaka, *J. Inorg. Biochem.*, 1984, **22**, 1873.
- 12 G. W. Watt and J. Chrips, *Anal. Chem.*, 1952, **24**, 2066.
- 13 K. Tanaka, M. Moriya, and T. Tanaka, *Chem. Lett.*, 1987, 373; *Inorg. Chem.*, 1988, **27**, 137.
- 14 R. J. Burt, G. J. Leigh, and C. J. Pickett, *J. Chem. Soc., Chem. Commun.*, 1976, 940.
- 15 R. F. Lane and A. T. Hubbard, *J. Phys. Chem.*, 1973, **77**, 1401; E. Laviron, *J. Electroanal. Chem.*, 1979, **100**, 263; H. Angerstein-Kozłowska, J. Klinger, and B. E. Conway, *ibid.*, 1977, **75**, 45.
- 16 E. J. Laskowski, R. B. Frankel, W. O. Gillum, G. C. Papaefthymiou, J. Renaud, J. A. Ibers, and R. H. Holm, *J. Am. Chem. Soc.*, 1978, **100**, 5322.
- 17 G. N. Schrauzer, G. W. Keifer, K. Tano, and P. A. Doemeny, *J. Am. Chem. Soc.*, 1974, **96**, 641.
- 18 Z. Dori and R. F. Ziolo, *Chem. Rev.*, 1973, **73**, 247.
- 19 A. Mertens, K. Lammertsma, M. Arvanaghi, and G. A. Olah, *J. Am. Chem. Soc.*, 1985, **105**, 5657.
- 20 E. J. Kaufmann and R. C. Thompson, *J. Am. Chem. Soc.*, 1979, **99**, 1824; M. Nitta and T. Kobayashi, *Bull. Chem. Soc. Jpn.*, 1984, **57**, 1035.
- 21 G. L. Hillhouse and B. L. Haymore, *J. Organomet. Chem.*, 1978, **162**, C23.
- 22 K. Burgess, B. F. G. Johnson, J. Lewis, and P. R. Raithby, *J. Organomet. Chem.*, 1982, **224**, C40.
- 23 G. L. Hillhouse and J. Bercaw, *Organometallics*, 1982, **1**, 1025.

Received 18th March 1988; Paper 8/01110I